metals

MDPI

Article

Phase Equilibria of the Co-Ti-Ta Ternary System

Cuiping Wang [1,*], Xianjie Zhang [1], Lingling Li [1], Yunwei Pan [1], Yuechao Chen [1], Shuiyuan Yang [1], Yong Lu [1], Jiajia Han [1] and Xingjun Liu [1,2,*]

1 College of Materials and Fujian Key Laboratory of Materials Genome, Xiamen University, Xiamen 361005, China; zhang779330597@163.com (X.Z.); xmulee@foxmail.com (L.L.); ywpan@stu.xmu.edu.cn (Y.P.); cycofxmu@foxmail.com (Y.C.); yangshuiyuan@xmu.edu.cn (S.Y.); luyong@xmu.edu.cn (Y.L.); jiajiahan@xmu.edu.cn (J.H.)

2 State Key Laboratory of Advanced Welding and Joining, Harbin Institute of Technology, Shenzhen 518005, China

* Correspondence: wangcp@xmu.edu.cn (C.W.); lxj@xmu.edu.cn (X.L.); Tel.: +86-592-2187888 (X.L.); Fax: +86-592-2187966 (C.W.)

Received: 29 October 2018; Accepted: 14 November 2018; Published: 16 November 2018

Abstract: The phase equilibria of the Co-Ti-Ta ternary system at 1000 °C, 1100 °C, and 1200 °C were experimentally investigated using an electron probe microanalyzer and X-ray diffraction. Experimental results show that: (1) No ternary compound exists in the studied isothermal sections; (2) the β(Ti) and β(Ta) phases form the continuous solid solution β(Ti,Ta) in the Ti-Ta side; (3) the solubility of Ta in the (αCo) is less than 5%; (4) the phases of Co_2Ti(h) and γ-Co_2Ta, Co_2Ti(c) and β-Co_2Ta form the continuous solid solutions Co_2(Ta,Ti)(h) and Co_2(Ta,Ti)(c), respectively.

Keywords: Co-Ti-Ta; isothermal section; phase equilibria

1. Introduction

Since Sato et al. [1] reported the metastable $L1_2$ structure Co_3(Al,W) phase, Co-based superalloys strengthened by γ'-Co_3X phase with an ordered $L1_2$ structure got researchers' attention again. Some reports have confirmed that the γ'-Co_3Ti phase has a stable $L1_2$ structure [2]. So researchers [3,4] have focused on the γ/γ' in the Co-Ti-X system, and found that the addition of elements Cr and V can distinctly improve strength above 600 °C, surpassing that of Co-9Al-8W and conventional Co-based superalloys. Furthermore, Ta is an important alloying element in both Co-based and Ni-based superalloys, in which Ta can stabilize the γ' phase [5,6]. Ta mainly substitutes Ti in the $L1_2$ type Co_3Ti phase [6], which makes the Co_3Ti phase more stable. Therefore, information on the phase equilibria in the Co-Ti-Ta system is important for Co-based superalloys. However, information on the phase equilibria of the Co-Ti-Ta system is very limited. Up to now, only Xu et al. [7] have studied the phase equilibria in the Co-Ti-Ta system at 950 °C, and Jiang et al. [8] reported knowledge of the Co-Ti-Ta and the phase relationship in the Co-rich region. These are not enough to understand the phase relationship in the Co-Ti-Ta system, especially phase equilibria at high temperatures. In the present work, phase equilibria of the Co-Ti-Ta ternary system at 1000 °C, 1100 °C, and 1200 °C, and the corresponding microstructure of Co-Ti-Ta alloys were investigated.

Three binary systems of Co-Ta [9–14], Co-Ti [15–20], and Ta-Ti [21] constituting the Co-Ta-Ti ternary system are shown in Figure 1. Six intermediate phases are known in the Co-Ta system, namely by μ-Co_6Ta_7, $CoTa_2$, α-Co_2Ta, β-Co_2Ta, γ-Co_2Ta, and Co_7Ta_2. The Co-Ti system has five intermediate phases, CoTi, $CoTi_2$(c), $CoTi_2$(h), Co_3Ti, and $CoTi_2$. The Ta-Ti system is a continuous solid solution, without any compounds. The stable solid phases and their crystal structures in all three binary systems are listed in Table 1.

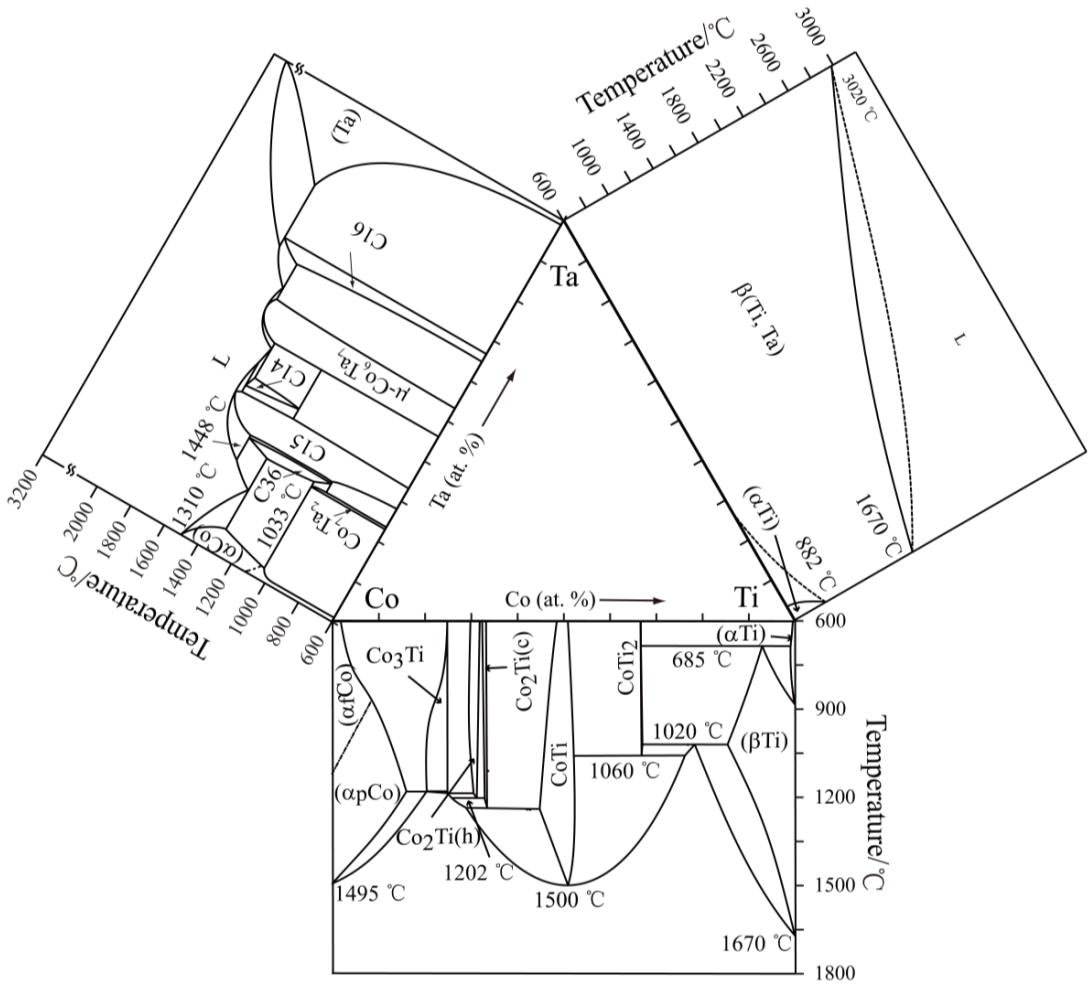

Figure 1. Binary phase diagrams constituting the Co-Ti-Ta ternary system [14,20,21].

Table 1. The stable solid phases in the Co-Ti-Ta ternary system.

System	Phase	Pearson's Symbol	Space Group	Prototype	Strukturbericht	References
Co-Ti	(αTi)	*hP2*	*P6₃/mmc*	Mg	*A3*	[20]
	(βTi)	*cI2*	*Im-3m*	W	*A2*	[20]
	$CoTi_2$	*cF96*	*Fd-3m*	Fe_3W_3C	$E9_3$	[20]
	CoTi	*cP2*	*Pm-3m*	CsCl	*B2*	[20]
	Co_2Ti(c)	*cF24*	*Fd-3m*	Cu_2Mg	*C15*	[20]
	Co_2Ti(h)	*hP24*	*P6₃/mmc*	$MgNi_2$	*C36*	[20]
	Co_3Ti	*cP4*	*Pm-3m*	Au_3Cu	$L1_2$	[20]
	(εCo)	*hP2*	*P6₃/mmc*	Mg	*A3*	[20]
	(αCo)	*cF4*	*Fm-3m*	Cu	*A1*	[20]
Co-Ta	Ta	*cI2*	*Im-3m*	W	*A2*	[14]
	Co_6Ta_7	*hR13*	*R-3m*	Fe_7W_6	$D8_b$	[14]
	$CoTa_2$	*tI12*	*I4/mcm*	Al_2Cu	*C16*	[14]
	α-Co_2Ta	*hP12*	*P6₃/mmc*	Zn_2Mg	*C14*	[14]
	β-Co_2Ta	*cF24*	*Fd-3m*	Cu_2Mg	*C15*	[14]
	γ-Co_2Ta	*hP24*	*P6₃/mmc*	$MgNi_2$	*C36*	[14]
	Co_7Ta_2	*hR36*	*R-3m*	$BaPb_3$	–	[14]
	(εCo)	*hP2*	*P6₃/mmc*	Mg	*A3*	[14]
	(αCo)	*cF4*	*Fm-3m*	Cu	*A1*	[14]
Ti-Ta	β(Ti,Ta)	*cI2*	*Im-3m*	W	*A2*	[21]

2. Experimental Procedures

Raw materials were from pure elements of cobalt (99.9 wt.%), titanium (99.9 wt.%), and tantalum (99.9 wt.%). Bulk alloys were prepared using an arc furnace (DHL-1, SKY Technology Development Co., Ltd, Shenyang, China), with non-consumable tungsten electrode under high purity argon atmosphere. In order to improve the homogeneity of the sample, the buttons were remelted four times. The weight loss of the alloys after melting did not exceed 0.5%. The samples for heat treatment were cut using a wire-cutting machine.

Vacuum in the quartz capsule containing alloys was pumped to 5 Pa, then filled with high purity argon at a certain pressure. To avoid oxidation of the samples, this process was repeated four times. The samples sealed in the quartz capsule were annealed at 1000 °C for 45 days, 1100 °C for 35 days or 8 h, and 1200 °C for 25 days or 8 h.

After annealing and metallographic preparation, the microstructure images of alloys and the equilibrium composition of each phase were observed and measured by an electron probe micro-analyzer (EPMA, JXA-8100R, JEOL, Tokyo, Japan). The measurements were taken at a voltage of 20 kV and a current of 1.0×10^{-8} A, with the measured results calibrated by ZAF (Z: Atomic number effect; A: Absorption effect; F: Fluorescence effect) correction. In order to reduce errors, the composition of each phase was determined by measuring five points, and then the final values were the average. Compositions of the liquid phase were determined via area analysis using the EDS (Energy Dispersive Spectroscopy) (INCA x-sight 7412, Oxford instruments, London, UK) at a voltage of 20 kV and a current of 2.0×10^{-9} A, with seven measurements. The constituent phases of the alloys were determined by XRD (X-ray diffraction) (Bruker Daltonic Inc., Billerica, MA, USA) on a Phillips Panalytical X-pert diffractometer using Cu Kα radiation at 40 kV and 40 mA. The data were collected in the range of 2θ from 20° to 90° at a step of 0.0167°.

3. Results and Discussion

3.1. Microstructure Morphology

BSE images of typical ternary Co-Ti-Ta alloys are presented in Figure 2a–j, and the XRD results of the typical ternary Co-Ti-Ta alloys are presented in Figure 3a–c.

Figure 2a presents the three-phase microstructure of the (αCo) + Co_3Ti + Co_7Ta_2 in the $Co_{80}Ti_9Ta_{11}$ (at.%) alloy annealed at 1000 °C for 45 days. Figure 2b shows the three-phase microstructure of the $CoTi_2$ + CoTi + β(Ti,Ta) in the $Co_{30}Ti_{50}Ta_{20}$ (at.%) alloy annealed at 1000 °C for 45 days. The crystal structures of three phases were identified by the XRD in Figure 3a, the characteristic peaks of three phases are marked by different symbols. The two-phase equilibrium of the Co_3Ti + Co_2(Ta,Ti)(h) was identified in the $Co_{71}Ti_{28}Ta_1$ (at.%) alloy annealed at 1000 °C for 45 days, as shown in Figure 2c. Figure 2d presents the two-phase microstructure of the CoTi + Co_2(Ta,Ti) (c) in the $Co_{60}Ti_{30}Ta_{10}$ (at.%) alloy annealed at 1100 °C for 35 days. The two-phase microstructure of the CoTi + Liquid (L) in the $Co_{40}Ti_{58}Ta_2$ (at.%) alloy annealed at 1100 °C for 8 h, shown in Figure 2e. Figure 2f presents the three-phase microstructure of the CoTi + β(Ti,Ta) + Liquid(L) in the $Co_{30}Ti_{50}Ta_{20}$ (at.%) alloy annealed at 1100 °C for 8 h. After annealing at 1200 °C for 8 h of the $Co_{85}Ti_{13}Ta_2$ (Figure 2g), the two-phase microstructure of the (αCo) + Liquid(L) was observed. The three-phase equilibrium of the CoTi + Co_2(Ta,Ti)(c) + Co_6Ta_7 was identified in the $Co_{55}Ti_{15}Ta_{30}$ (at.%) alloy annealed at 1200 °C for 25 days, as shown in Figure 2h. Figure 2i presents the three-phase microstructure of the CoTi + Co_6Ta_7 + $CoTa_2$ in the $Co_{45}Ti_{15}Ta_{40}$ (at.%) alloy annealed at 1200 °C for 25 days, its XRD result is shown in Figure 3b. Figure 2j shows the three-phase microstructure of the $CoTa_2$ + CoTi + β(Ti,Ta) in the $Co_{30}Ti_{20}Ta_{50}$ (at.%) alloy annealed at 1200 °C for 25 days, its XRD result is shown in Figure 3c.

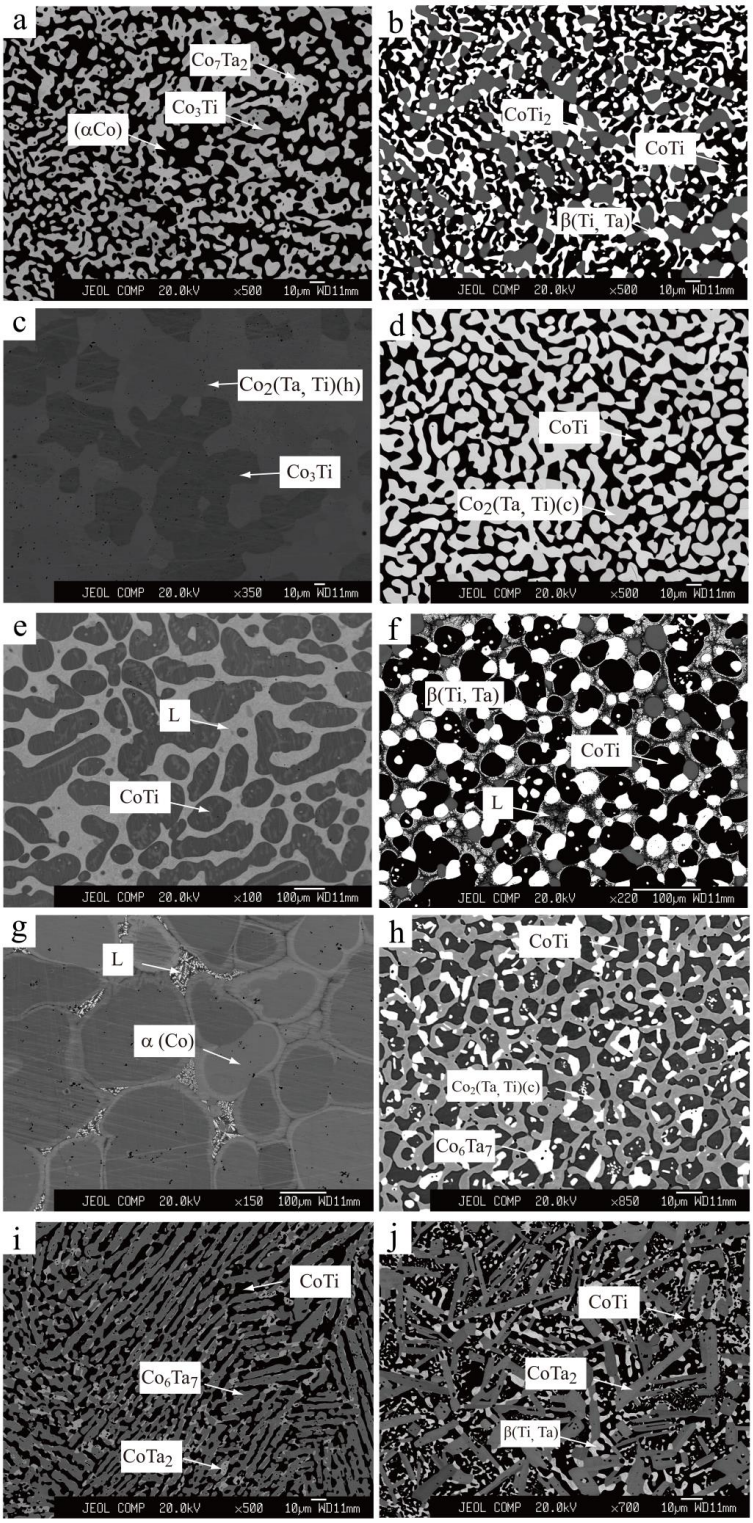

Figure 2. Typical ternary BSE (Back scattered Electron) images obtained from: (**a**) $Co_{80}Ti_9Ta_{11}$ alloy annealed at 1000 °C for 45 days; (**b**) $Co_{30}Ti_{50}Ta_{20}$ alloy annealed at 1000 °C for 45 days; (**c**) $Co_{71}Ti_{28}Ta_1$ alloy annealed at 1000 °C for 45 days; (**d**) $Co_{60}Ti_{30}Ta_{10}$ alloy annealed at 1100 °C for 35 days; (**e**) $Co_{40}Ti_{58}Ta_2$ alloy annealed at 1100 °C for 8 h; (**f**) $Co_{30}Ti_{50}Ta_{20}$ alloy annealed at 1100 °C for 8 h; (**g**) $Co_{85}Ti_{13}Ta_2$ alloy annealed at 1200 °C for 25 days; (**h**) $Co_{55}Ti_{15}Ta_{30}$ alloy annealed at 1200 °C for 25 days; (**i**) $Co_{45}Ti_{15}Ta_{40}$ alloy annealed at 1200 °C for 25 days; and (**j**) $Co_{30}Ti_{20}Ta_{50}$ alloy annealed at 1200 °C for 25 days.

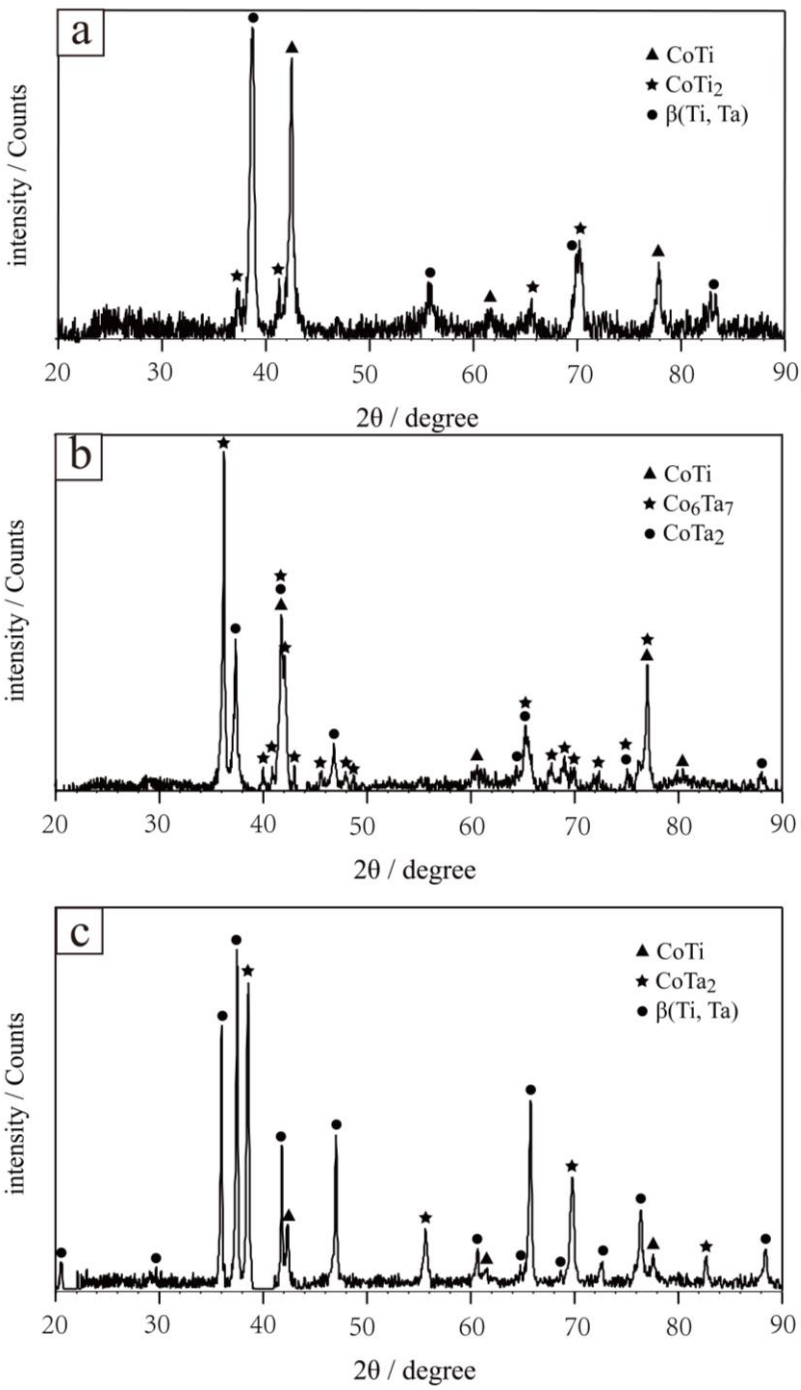

Figure 3. X-ray diffraction patterns obtained from: (**a**) $Co_{30}Ti_{50}Ta_{20}$ alloy annealed at 1000 °C for 45 days; (**b**) $Co_{45}Ti_{15}Ta_{40}$ alloy annealed at 1100 °C for 35 days; and (**c**) $Co_{30}Ti_{20}Ta_{50}$ alloy annealed at 1100 °C for 35 days.

3.2. Isothermal Sections

The equilibrium compositions of the Co-Ti-Ta ternary system in this study at 1000 °C, 1100 °C, and 1200 °C determined by EPMA are summarized in Tables 2–4. Based on the obtained experimental data mentioned above, the isothermal sections at 1000 °C, 1100 °C, and 1200 °C have been constructed in Figure 4a–c. Undetermined three-phase equilibria are labeled in the dashed lines.

Table 2. Equilibrium composition of the Co-Ti-Ta ternary system at 1000 °C determined in the present work.

Alloys (at.%)	Annealed Time	Equilibria	Composition (at.%)					
		Phase 1/Phase 2/Phase 3	Phase 1		Phase 2		Phase 3	
			Ta	Ti	Ta	Ti	Ta	Ti
$Co_{85}Ti_{13}Ta_2$	45 days	(αCo)/Co_3Ti	1.0	10.8	3.0	17.1	—	—
$Co_{85}Ti_2Ta_{13}$	45 days	(αCo)/Co_7Ta_2	0.9	2.3	1.0	22.5	—	—
$Co_{80}Ti_9Ta_{11}$	45 days	(αCo)/Co_3Ti/Co_7Ta_2	2.1	5.3	11.5	10.3	16.4	7.7
$Co_{71}Ti_{28}Ta_1$	45 days	Co_3Ti/Co_2(Ti,Ta)(h)	0.8	24.1	1.3	28.7	—	—
$Co_{74}Ti_{16}Ta_{10}$	45 days	Co_3Ti/Co_7Ta_2/Co_2(Ti,Ta)(h)	7.0	15.8	8.4	15.3	10.5	15.4
$Co_{74}Ti_{10}Ta_{16}$	45 days	(αCo)/Co_7Ta_2	2.1	4.2	19.2	5.1	—	—
$Co_{75}Ti_1Ta_{14}$	45 days	Co_2(Ti,Ta)(h)	23.1	0.6	—	—	—	—
$Co_{60}Ti_2Ta_{38}$	45 days	Co_2(Ti,Ta)(c)/Co_6Ta_7	31.5	2.1	43.2	1.8	—	—
$Co_{55}Ti_{15}Ta_{30}$	45 days	Co_2(Ti,Ta)(c)/Co_6Ta_7/CoTi	28.4	8.1	39.9	6.0	20.8	27.6
$Co_{60}Ti_{30}Ta_{10}$	45 days	Co_2(Ti,Ta)(c)/CoTi	10.8	19.4	4.5	41.6	—	—
$Co_{45}Ti_{15}Ta_{40}$	45 days	CoTi/Co_6Ta_7/$CoTa_2$	19.8	30.3	47.1	7.9	53.2	7.9
$Co_{30}Ti_{20}Ta_{50}$	45 days	CoTi/$CoTa_2$/β(Ti,Ta)	8.1	43.7	55.6	9.8	86.0	8.3
$Co_{30}Ti_{50}Ta_{20}$	45 days	CoTi/$CoTi_2$/β(Ti,Ta)	2.1	43.3	6.3	61.4	51.3	42.5
$Co_{40}Ti_{58}Ta_2$	45 days	CoTi/$CoTi_2$	1.1	51.1	3.5	64.1	—	—
$Co_{80}Ti_{15}Ta_5$	45 days	(αCo)/Co_3Ti	1.0	9.5	5.7	16.1	—	—
$Co_{62}Ti_{20}Ta_{18}$	45 days	Co_2(Ti,Ta)(c)/CoTi	22.3	11.9	11.3	35.7	—	—
$Co_{20}Ti_{75}Ta_5$	45 days	$CoTi_2$/β(Ti,Ta)	2.0	65.0	6.2	78.8	—	—
$Co_{42}Ti_3Ta_{55}$	45 days	Co_6Ta_7/$CoTa_2$	52.0	3.0	57.5	3.5	—	—
$Co_{30}Ti_{40}Ta_{30}$	45 days	CoTi/β(Ti,Ta)	3.1	46.2	71.2	22.9	—	—

Table 3. Equilibrium composition of the Co-Ti-Ta ternary system at 1100 °C determined in the present work.

Alloys (at.%)	Annealed Time	Equilibria	Composition (at.%)					
		Phase 1/Phase 2/Phase 3	Phase 1		Phase 2		Phase 3	
			Ta	Ti	Ta	Ti	Ta	Ti
$Co_{85}Ti_{13}Ta_2$	35 days	(αCo)/Co_3Ti	1.6	11.5	5.9	11.6	—	—
$Co_{80}Ti_5Ta_{15}$	35 days	(αCo)/Co_2(Ti,Ta)(h)	2.7	5.6	18.7	6.7	—	—
$Co_{85}Ti_2Ta_{13}$	35 days	(αCo)/Co_2(Ti,Ta)(h)	3.6	1.3	22.4	1.2	—	—
$Co_{71}Ti_{28}Ta_1$	35 days	Co_3Ti/Co_2(Ti,Ta)(h)	0.6	23.8	1.0	28.7	—	—
$Co_{74}Ti_{16}Ta_{10}$	35 days	(αCo)/Co_3Ti/Co_2(Ti,Ta)(h)	1.7	10.5	6.9	16.2	10.8	15.9
$Co_{74}Ti_{10}Ta_{16}$	35 days	(αCo)/Co_2(Ti,Ta)(h)	2.4	8.3	15.2	10.9	—	—
$Co_{75}Ti_1Ta_{24}$	35 days	Co_2(Ti,Ta)(h)	23.2	0.9	—	—	—	—
$Co_{60}Ti_2Ta_{38}$	35 days	Co_2(Ti,Ta)(c)/Co_6Ta_7	31.4	2.2	44.7	1.9	—	—
$Co_{55}Ti_{15}Ta_{30}$	35 days	Co_2(Ti,Ta)(c)/Co_6Ta_7/CoTi	29.6	8.0	41.1	6.3	23.3	26.3
$Co_{60}Ti_{30}Ta_{10}$	35 days	Co_2(Ti,Ta)(c)/CoTi	11.6	22.7	5.5	41.1	—	—
$Co_{45}Ti_{15}Ta_{40}$	35 days	CoTi/Co_6Ta_7/$CoTa_2$	21.4	29.6	46.4	8.3	61.3	3.7
$Co_{30}Ti_{20}Ta_{50}$	35 days	CoTi/$CoTa_2$/β(Ti,Ta)	16.8	38.5	56.6	9.9	86.1	9.9
$Co_{30}Ti_{50}Ta_{20}$	8 h	CoTi/Liquid/β(Ti,Ta)	2.9	50.0	4.5	68.3	45.9	48.8
$Co_{40}Ti_{58}Ta_2$	8 h	CoTi/Liquid	1.0	51.7	2.7	69.2	—	—
$Co_{15}Ti_{84}Ta_1$	8 h	Liquid/β(Ti,Ta)	0.7	78.8	2.0	88.0	—	—
$Co_{62}Ti_{20}Ta_{18}$	35 days	Co_2(Ti,Ta)(c)/CoTi	20.6	12.8	12.3	34.0	—	—
$Co_{20}Ti_{75}Ta_5$	8 h	Liquid/β(Ti,Ta)	4.0	73.9	7.3	82.7	—	—
$Co_{42}Ti_3Ta_{55}$	35 days	Co_6Ta_7/$CoTa_2$	52.9	3.0	63.1	1.6	—	—
$Co_{30}Ti_{40}Ta_{30}$	35 days	CoTi/β(Ti,Ta)	3.9	48.5	66.7	28.9	—	—

Figure 4a shows the isothermal section at 1000 °C, six three-phase regions were experimentally determined as follows: (αCo) + Co_3Ti + Co_7Ta_2, Co_3Ti + Co_7Ta_2 + Co_2(Ta,Ti)(h), Co_2(Ta,Ti)(c) + Co_6Ta_7 + CoTi, $CoTa_2$ + Co_6Ta_7 + CoTi, $CoTa_2$ + β(Ti,Ta) + CoTi, CoTi + $CoTi_2$ + β(Ti,Ta). The results show that: (1) The solubilities of Ta in the CoTi, and Co_3Ti were 21%, and 12%, respectively. (2) The solubility of Ti in the Co_7Ta_2 was 9%. (3) The phases of Co_2Ti (h) and γ-Co_2Ta, Co_2Ti (c) and β-Co_2Ta formed continuous solid solutions.

There are five three-phase regions in the isothermal section at 1100 °C in Figure 4b, including the (αCo) + Co_3Ti + Co_2(Ta,Ti)(h), Co_2(Ta,Ti)(c) + Co_6Ta_7 + CoTi, $CoTa_2$ + Co_6Ta_7 + CoTi, $CoTa_2$ + β(Ti,Ta) + CoTi, and CoTi + Liquid + β(Ti,Ta). In the isothermal section at 1100 °C, the phases of Co_7Ta_2 and $CoTi_2$ disappeared and the liquid phase presented.

Table 4. Equilibrium composition of the Co-Ti-Ta ternary system at 1200 °C determined in the present work.

Alloys (at.%)	Annealed Time	Equilibria	Composition (at.%)					
		Phase 1/Phase 2/Phase 3	Phase 1		Phase 2		Phase 3	
			Ta	Ti	Ta	Ti	Ta	Ti
$Co_{85}Ti_{13}Ta_2$	8 h	(αCo)/Liquid	1.2	11.4	2.1	17.2	—	—
$Co_{85}Ti_2Ta_{13}$	25 days	(αCo)/Co_2(Ti,Ta) (h)	4.7	1.2	22.5	1.0	—	—
$Co_{80}Ti_9Ta_{11}$	25 days	(αCo)/Co_2(Ti,Ta)(h)	3.2	7.2	16.5	8.6	—	—
$Co_{71}Ti_{28}Ta_1$	8 h	Liquid/Co_2(Ti,Ta)(h)	0.1	23.2	0.9	30.2	—	—
$Co_{74}Ti_{16}Ta_{10}$	8 h	Liquid/Co_2(Ti,Ta)(h)	3.1	18.5	9.9	17.4	—	—
$Co_{60}Ti_2Ta_{38}$	25 days	Co_2(Ti,Ta)(c)/Co_6Ta_7	32.5	1.0	44.4	0.8	—	—
$Co_{55}Ti_{15}Ta_{30}$	25 days	Co_2(Ti,Ta)(c)/Co_6Ta_7/CoTi	30.4	7.5	40.7	5.4	26.0	22.0
$Co_{60}Ti_{32}Ta_8$	25 days	Co_2(Ti,Ta)(c)/CoTi	10.3	20.3	5.9	37.7	—	—
$Co_{45}Ti_{15}Ta_{40}$	25 days	CoTi/Co_6Ta_7/$CoTa_2$	25.2	24.1	45.1	7.0	60.3	3.8
$Co_{30}Ti_{50}Ta_{20}$	8 h	CoTi/Liquid/β(Ti,Ta)	5.5	46.5	7.7	63.2	49.5	43.5
$Co_{40}Ti_{58}Ta_2$	8 h	CoTi/Liquid	1.0	49.8	2.7	67.6	—	—
$Co_{14}Ti_{84}Ta_2$	8 h	Liquid/β(Ti,Ta)	1.5	84.5	2.5	89.2	—	—
$Co_{80}Ti_{15}Ta_5$	8 h	(αCo)/Liquid/Co_2(Ti,Ta)(h)	2.1	11.7	3.8	16.0	10.0	16.2
$Co_{60}Ti_{20}Ta_{20}$	25 days	Co_2(Ti,Ta)(c)/CoTi	19.1	14.2	12.3	32.5	—	—
$Co_{75}Ti_6Ta_{19}$	25 days	(αCo)/Co_2(Ti,Ta)(h)	3.9	4.4	19.2	4.7	—	—
$Co_{42}Ti_3Ta_{55}$	25 days	Co_6Ta_7/$CoTa_2$	52.9	3.0	63.1	1.6	—	—
$Co_{30}Ti_{40}Ta_{30}$	25 days	CoTi/β(Ti,Ta)	6.6	44.7	74.2	23.2	—	—

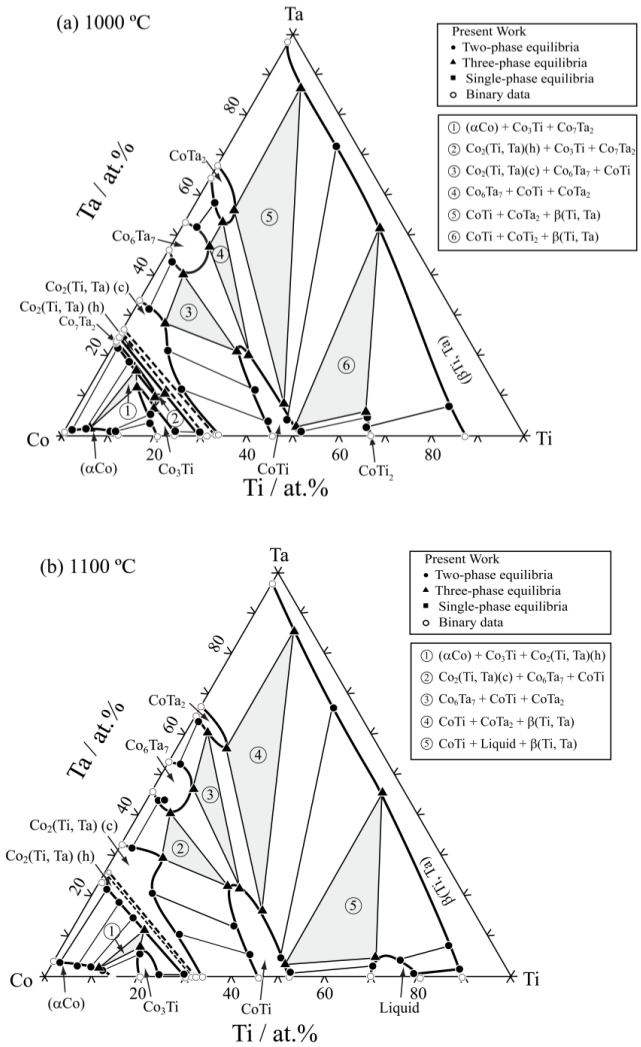

Figure 4. *Cont.*

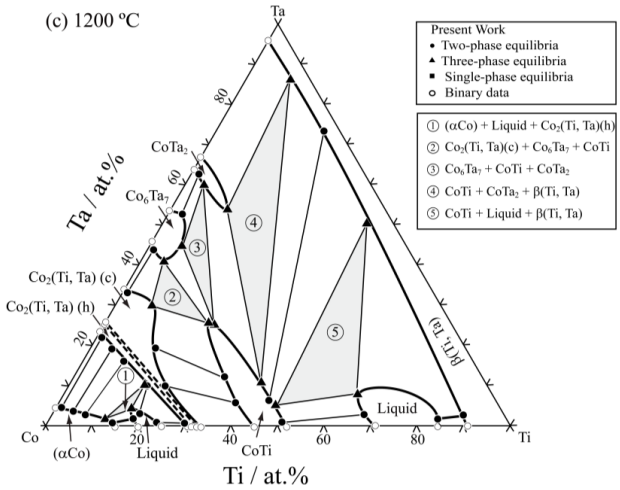

Figure 4. Experimentally determined isothermal sections of the Co-Ti-Ta system at: (**a**) 1000 °C; (**b**) 1100 °C; and (**c**) 1200 °C.

In the isothermal section at 1200 °C shown in Figure 4c, five three-phase regions of (αCo) + Liquid + Co_2(Ta,Ti)(h), Co_2(Ta,Ti)(c) + Co_6Ta_7 + CoTi, $CoTa_2$ + Co_6Ta_7 + CoTi, $CoTa_2$ + β(Ti,Ta) + CoTi,CoTi + Liquid + β(Ti,Ta) were completely obtained. When the temperature increased from 1100 °C to 1200 °C, the Co_3Ti phase decomposed while a liquid phase appeared. The solubility of Ta in the CoTi phase increased to 26%, and the solubility of Ti in the $CoTa_2$ increased to 12%.

Compared with the previous phase equilibria information on Co-Ti-Ta [7,8], we find that the results are consistent with the experimental results conducted by Xu [7] and Jiang [8]. Combining phase equilibria information of Co-Ti-Ta at the isothermal section 950 °C, which were obtained by Xu [7] (Figure 5), it was found that: (1) The phases of β(Ti) and β(Ta) form the continuous solid solution β(Ti,Ta); (2) the phases of Co_2Ti(h) and γ-Co_2Ta, Co_2Ti (c) and β-Co_2Ta form the continuous solid solutions Co_2(Ta,Ti)(h) and Co_2(Ta,Ti) (c), respectively; (3) the solubility of Ta in the Co_3Ti decreases from 950 °C to 1100 °C, but the Co_3Ti phase is absent at 1200 °C; (4) the Co_7Ta_2 does not exist in 1100 °C and 1200 °C, but it exists at 1000 °C with about 9% of the solubility of Ta; (5) a liquid phase region arises near the Ti-rich corner at 1100 °C and 1200 °C.

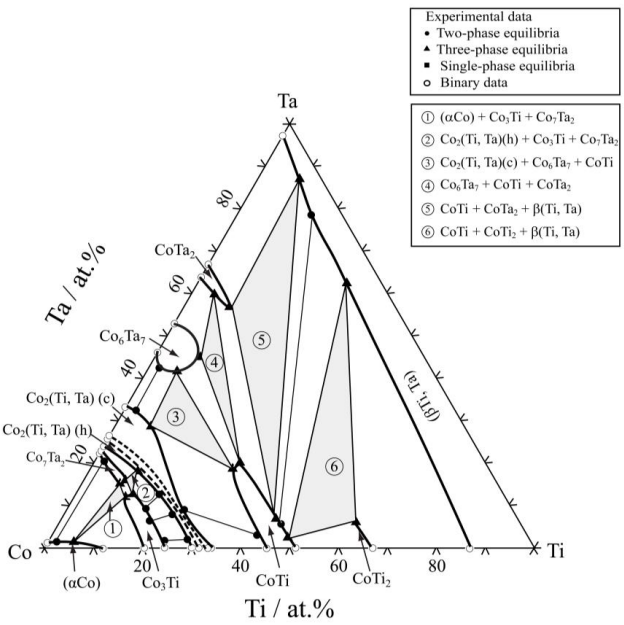

Figure 5. Experimentally determined isothermal sections of the Co-Ti-Ta system at 950 °C by Xu [7].

4. Conclusions

In the present study, three isothermal sections of the Co-Ti-Ta ternary alloys at 1000 °C, 1100 °C, and 1200 °C were determined by EPMA and XRD. The results show: (1) No ternary compound exists in the isothermal sections at 1000–1200 °C; (2) the β(Ti) and β(Ta) phases form the continuous solid solution β(Ti,Ta) in the Ti-Ta side; (3) the solubility of Ta in the (αCo) is less than 5%; (4) the phases of Co_2Ti(h) and γ-Co_2Ta, Co_2Ti (c) and β-Co_2Ta form the continuous solid solutions Co_2(Ta,Ti)(h) and Co_2(Ta,Ti)(c), respectively.

Author Contributions: Conceptualization, C.W. and X.L.; investigation, X.Z. and Y.C.; writing and original draft preparation, X.Z., Y.L. and J.H.; writing, reviewing and editing, Y.P., L.L. and S.Y.; supervision, X.L. and C.W.; and funding acquisition, X.L. and C.W.

Funding: This work was supported by the National Key R&D Program of China (Grant No. 2016YFB0701401), and the Natural Science Foundation of China (Grant No. 51471138 and 51571168).

Conflicts of Interest: The authors declare no conflict of interest.

References

1. Sato, J.; Omori, T.; Oikawa, K.; Ohnuma, I.; Kainuma, R.; Ishida, K. Cobalt-base high-temperature alloys. *Science* **2006**, *312*, 90–91. [CrossRef] [PubMed]
2. Blaise, J.M.; Viatour, P.; Drapier, J.M. On the stability and precipitation of the Co3Ti phase in Co-Ti alloys. *Cobalt* **1970**, *49*, 192–195.
3. Zenk, C.H.; Povstugar, I.; Li, R.F.; Neumeier, S.; Raabe, D.; Gökena, M. A novel type of Co–Ti–Cr-base γ/γ' superalloys with low mass density. *Acta Mater.* **2017**, *135*, 244–251. [CrossRef]
4. Ruan, J.J.; Wang, C.P.; Zhao, C.C.; Yang, S.Y.; Yang, T.; Liu, X.J. Experimental investigation of phase equilibria and microstructure in the Co-Ti-V ternary system. *Intermetallics* **2014**, *49*, 121–131. [CrossRef]
5. Jia, C.C.; Ishida, K.; Nishizawa, T. Partition of alloying elements between γ(A1), $\gamma'(L1_2)$, and β(B2) phases in Ni-Al base systems. *Metall. Mater. Trans. A* **1994**, *25*, 473–485. [CrossRef]
6. Ooshima, M.; Tanaka, K.; Okamoto, N.L.; Kishida, K.; Inui, H. Effects of quaternary alloying elements on the γ' solvus temperature of Co-Al-W based alloys with fcc/$L1_2$ two-phase microstructures. *J. Alloys Compd.* **2010**, *508*, 71–78. [CrossRef]
7. Xu, H.; Xiong, X.; Du, Y.; Wang, P.; Hu, B.; He, Y. Phase equilibria of the Co-Ta-Ti system at 950 °C. *J. Alloys Compd.* **2009**, *485*, 249–254. [CrossRef]
8. Jiang, M.; Saren, G.; Yang, S.; Li, H.; Hao, S. Phase equilibria in Co-rich region of Co-Ti-Ta system. *Trans. Nonferr. Met. Soc. China* **2011**, *21*, 2391–2395. [CrossRef]
9. Pet'kov, V.V.; Kocherzhinskii, Y.A.; Markiv, V.Y. Investigations of the phase diagram in the system ta-co. *Metall. Akad. Nauk Ukr. Inst. Metall.* **1972**, *41*, 93–97.
10. Kaufman, L. Coupled thermochemical and phase diagram data for tantalum based binary alloys. *Calphad* **1991**, *15*, 243–259. [CrossRef]
11. Liu, Z.K.; Chang, Y.A. Thermodynamic assessment of the Co-Ta system. *Calphad* **1999**, *23*, 339–356. [CrossRef]
12. Kumar, K.C.H.; Rompaey, T.V.; Wollants, P. Thermodynamic calculation of the phase diagram of the Co-Nb-Ta system. *Z. Metall.* **2002**, *93*, 1146–1153. [CrossRef]
13. Okamoto, H. Co-Ta (Cobalt-Tantalum). *J. Phase Equilib. Diffus.* **2004**, *25*, 571. [CrossRef]
14. Shinagawa, K.; Chinen, H.; Omori, T.; Oikawa, K.; Ohnuma, I.; Ishida, K.; Kniauma, R. Phase equilibria and thermodynamic calculation of the Co-Ta binary system. *Intermetallics* **2014**, *49*, 87–97. [CrossRef]
15. Huthmann, H.; Inden, G. High-temperature neutron diffraction on FeTi and CoTi. *Phys. Status Solidi A* **1975**, *28*, K129–K130. [CrossRef]
16. Kornilov, I.I.; Kachur, E.V.; Belousov, O.K. Study of the TiNi-TiCo System. *Izv. Akad Nauk Metall.* **1975**, *2*, 209–210.
17. Murray, J.L. The Co-Ti (Cobalt-Titanium) system. *Bull. Alloy Phase Diagrams* **1982**, *3*, 74–85. [CrossRef]
18. Nash, P.; Choo, H.; Schwarz, R.B. Thermodynamic calculation of phase equilibria in the Ti-Co and Ni-Sn systems. *J. Mater. Sci.* **1998**, *33*, 4929–4936. [CrossRef]
19. Cacciamani, G.; Ferro, R.; Ansara, I.; Dupin, N. Thermodynamic modelling of the Co-Ti system. *Intermetallics* **2000**, *8*, 213–222. [CrossRef]

20. Davydov, A.V.; Kattner, U.R.; Josell, D.; Waterstrat, R.M.; Boettinger, W.J.; Blendell, J.E.; Shapiro, A.J. Determination of the CoTi congruent melting point and thermodynamic reassessment of the Co-Ti system. *Metall. Mater. Trans. A* **2001**, *32*, 2175–2186. [CrossRef]
21. Murray, J.L. *Bulletin of Alloy Phase Diagram*, 2nd ed.; Springer: Berlin, Germany, 1981; pp. 62–66.